International Journal of Mechanical and Production Engineering Research and Development (IJMPERD)
ISSN(P): 2249-6890; ISSN(E): 2249-8001
Vol. 9, Issue 4, Aug 2019, 907-918

STRESS ANALYSIS OF A SPLICE JOINT IN AN AIRCRAFT FUSELAGE WITH THE PREDICTION OF FATIGUE LIFE TO CRACK INITIATION

SURESH R, SHYAMSUNDER N & DEVENDRA REDDY M

Assistant Professor, Department of Mechanical Engineering,

Sri Venkateshwara College of Engineering, Bangalore, India

ABSTRACT

The objective of this dissertation is to Stress analysis and prediction of fatigue life to crack initiation in an in a transport aircraft fuselage. Typical splice joint panel consisting of skin plates, doubler plate is considered for the study. Aluminium alloy 2024-T351 material is considered for all the structural elements of the panel. A two dimensional finite element-analysis will be carried out on the splice joint panel. A panel consisting of a splice joint of a fuselage is considered for the linear static analysis, and then applying loads and boundary conditions on it. Cyclic pressurization loading is considered.

KEYWORDS: Finite Element Model; Ultimate Tensile Stress; Degrees of Freedom; MSC Patran and Nastran & Airframe Structure

Received: May 22, 2019; **Accepted:** Jun 12, 2019; **Published:** Jul 13, 2019; **Paper Id.:** IJMPERDAUG201992

Original Article

INTRODUCTION

A complete airplane structure is manufactured from many parts which must be joined together to form subassemblies and then into form larger assemblies then finally assembled into a completed airplane. Connections between metal parts are required in most applications, and are a critical part of every design. Many parts of the completed airplane must be arranged so that usually joined by Bonded and mechanically fastened joints. Here considering permanent fasteners called rivets. Rivets are low cost, permanent fasteners well suited to automatic assembly operations. Initial cost of rivets is substantially lower than that of threaded fasteners because rivets are made in large volumes on high-speed heading machines, with little scrap loss and low Assembly costs.

The joining of parts by cylindrical fasteners passing through holes, rivets require that holes be made to receive them, which reduces the net cross section, and these holes must be very accurately aligned. Although rivets can be used in any orientation, enough clearance must exist to set them properly. A riveted joint is quickly made, and is easy to inspect.

Typical splice joint panel consisting of rivets, skin plates, doubler plate and stiffeners. The skin is attached to the longerons, bulkheads, and other structural members and carries part of the load. The fuselage skin thickness varies with the load carried and the stresses sustained at particular location. The stringers are smaller and lighter than longerons they have some rigidity but are chiefly used for giving shape and for attachment of skin. A doubler's function is to pick up load. The bulkheads and formers hold the stringers All of these join together to form a rigid fuselage framework. Stringers and longerons prevent tension and compression stresses from bending

the fuselage.

A probabilistic method was developed to model structural failure associated with widespread damage as a stochastic chain of crack initiation and growth, linkup, and final failure. Stress analysis of Splice joint panel is performed using a finite element method and the fatigue life is determined at a given time increment by using an algebraic Empirical relationship equations for total life of the structure by stress life approach.

In the present work the stress analysis and fatigue analysis carried out in a splice joint of transport aircraft fuselage to check the design for its strength and fatigue characteristics. For this analyzed structure considering the maximum stress region near rivet location. Distribution of fasteners loads and local stress field at rivet locations will be studied from analysis. And this paper describes the modifications required to correct the boundary effects of the panel. The fatigue analysis is carried out near maximum stress location region of rivet. This is accomplished by using CATIA V4 for modeling and Patran as pre and post Processor while Nastran is used as solver

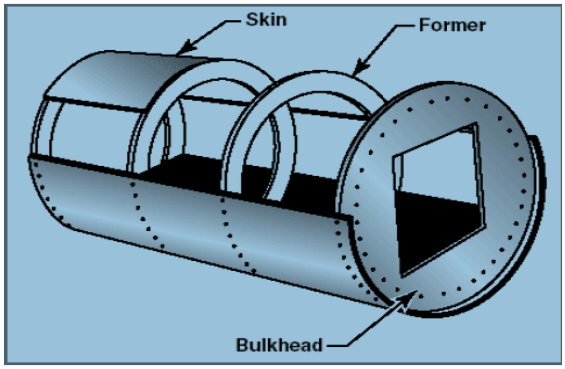

Figure 1.1: Fuselage Design

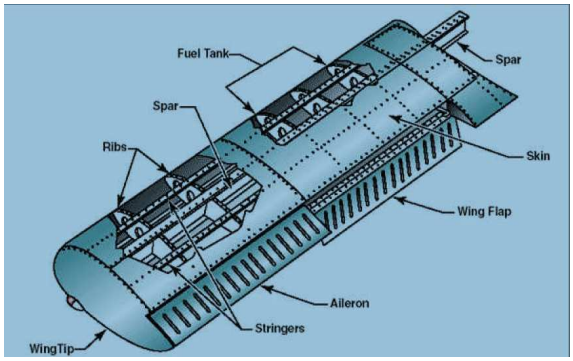

Figure 1.2: Wing Components

The ideal airframe would be a single complete unit of the same material involving one manufacturing operation. However, the majority of the present aluminum airframe structures consist of built-up construction. Also, the requirements of repair and maintenance dictate a structure of several main units held together by fastened joint subtilizing many rivets, bolts, bonding, lugs, fittings, etc

MATERIAL SELECTION, MODELING AND MESHING OF LUG JOINT

Aluminium alloy 2024 is an aluminium alloy, with copper and magnesium as the alloying elements. It is used in applications requiring high strength to weight ratio, as well as good fatigue resistance. It is not weldable, and has average machinability. Due to poor corrosion resistance, it is often clad with aluminium or Al-1Zn for protection, although this may

reduce the fatigue strength.

The material under investigation was a 2024-T351 aluminium alloy, with a chemical composition of (%): Si-0.05, Fe-0.5, Cu-3.8-4.9, Mn-0.3-0.9, Mg-1.2-1.8, Cr- O.I, Zn-0.25 and Ti-0.15. Mechanical properties of aluminium 2024-T351:T351 temper 2024 plate has following mechanical properties shown table:

Table 1: Mechanical Properties of 2024-T351

Modulus of elasticity GPa	70.3-72.4
Tensile strength MPa	470
Yield strength MPa	325
Hardness	120
Shear strength MPa	285
Fatigue limit , MPa,	140
Thickness in mm	6.35-101.60
Shear modules MPa	283
Elongation %	12-4

Geometric Dimensions of Fuselage Cabin

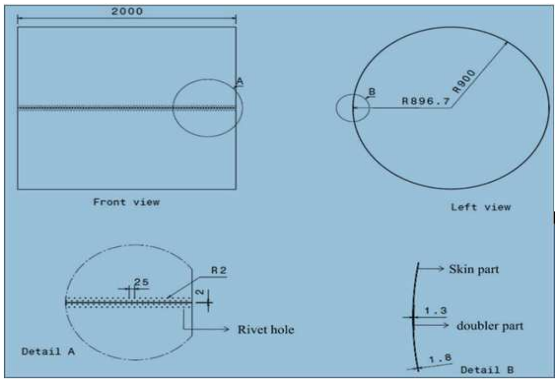

Figure 2.1: Shows the Geometric Model in 2D Drafting for Fuselage Cabin Contain Butt

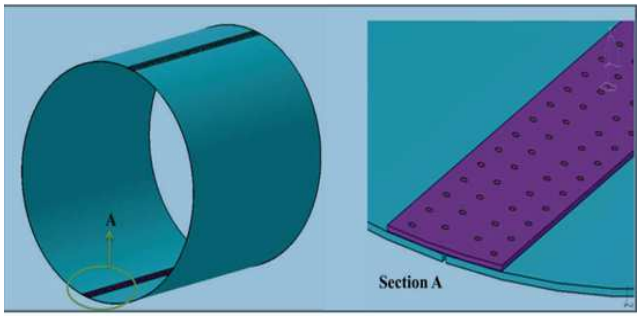

Figure 2.2: Shows the Geometric Model in 3D for Fuselage Cabin Contain Butt Joint

The components of fuselage cabin are idealized as shell elements and beam element and the type of elements used are CQUAD4 & CTRIA3 for skin and doubler. For rivets CBEAM used

Table 2: Details of Component and Type of Element

Component	Idealization	Type of Element
Skin	SHELL	CQUAD4 & CTRIA3
doubler	SHELL	CQUAD4
rivet	BEAM	CBEAM

Table 3: Total No of Nodes & Elements Used in Analysis

Type of Elements	No. of Elements
CQUAD4	43520
CTRIA3	960
CBEAM	636
Total no of elements	45116
Total no of nodes	45172

Loads Cases and Boundary Conditions of Fuselage Cabin

Boundary condition is application of force and constraint. It would be over enthusiastic to include an axially loaded called tensile load conditions. The end of finite element model fuselage cabin is constrained in both translational and rotational and we apply a uniform pressure of 6PSI to 9PSI on inner surface of fuselage called bottom pressure. Due to axially applied pressure load the skin and doubler or splice plate undergo tensile stresses and rivets also deform under axial load. Both translational and rotational constrained (X Y Z and R □ S) i. e. <0 0 0>

Design of Floor Beam (Bracket)

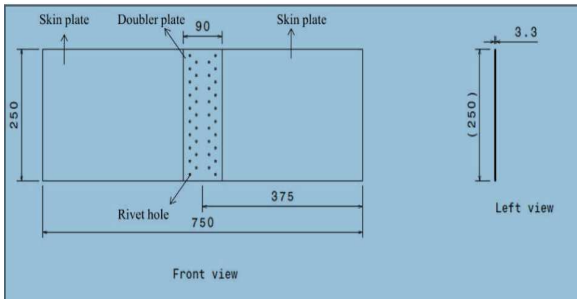

Figure 2.3: Shows the Geometric Model in 2D Drafting for Flat Panel Contains a Splice Joint with Dimensions

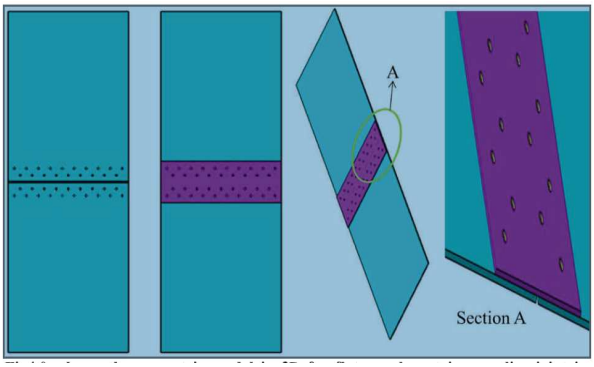

Figure 2.4: Shows the Geometric Model in 3D for Flat Panel Contains a Splice Joint in Different Views

The components of fuselage cabin are idealized as shell elements and beam element and the type of elements used are CQUAD4 & CTRIA3 for skin and doubler. For rivets CBEAM used

Table 4: Total No of Nodes & Elements Used in Analysis

Type of Elements	No. of Elements
CQUAD4	2240
CBEAM	28
Total no of elements	2278
Total no of nodes	3718

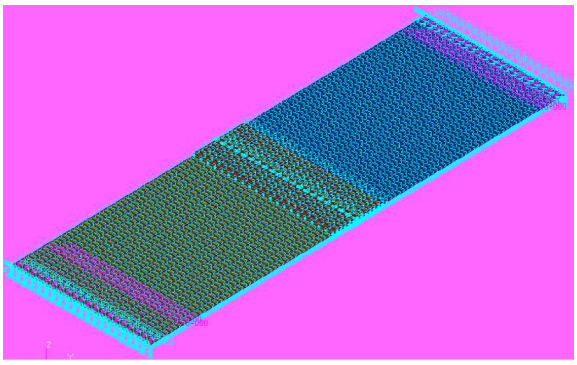

Figure 2.5: Global FE Model of Splice Joint Panel with Loads and Boundary Conditions

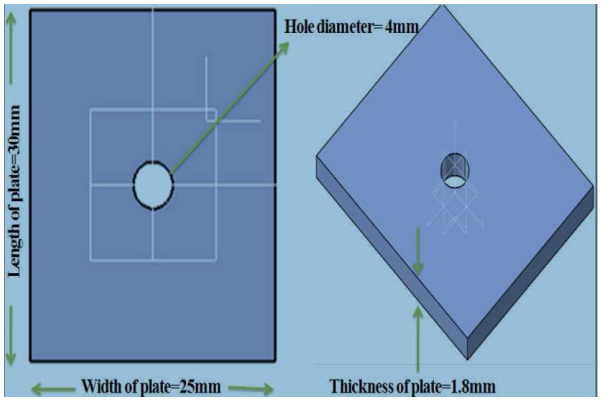

Figure 2.6: Shows the Geometric Model of Plate with Hole

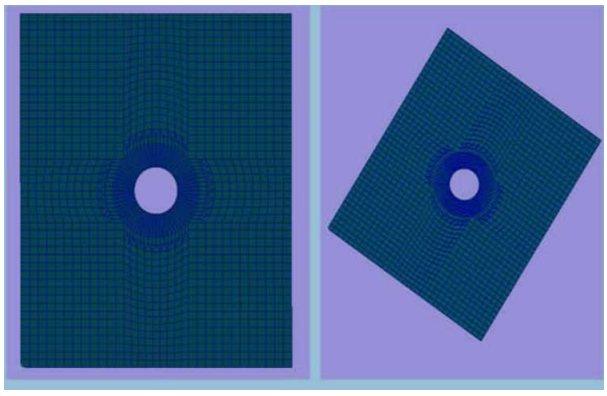

Figure 2.7: Shows the Meshed Plate with Hole

Table 5: Details of Component and Type of Element

Component	Idealization	Type of Element
Plate with hole	SHELL	CQUAD4 & CTRIA3

Table 6: Total No of Nodes & Elements Used in Analysis

Type of Elements	No. of Elements
CQUAD4	2196
CBEAM	102
Total no of elements	2298
Total no of nodes	2358

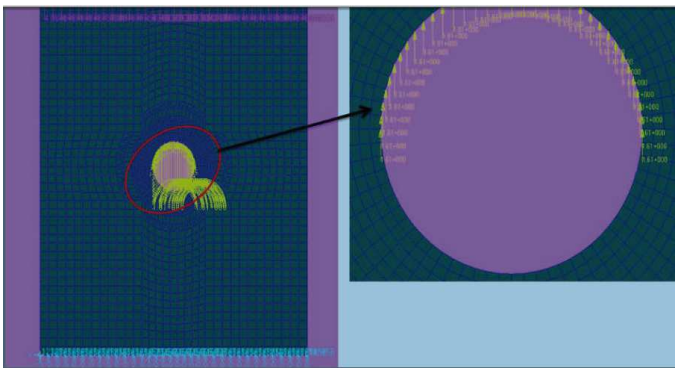

Figure 2.8: Shows Loads and Boundary Conditions Applied at Plate End and Hole Location

RESULTS AND DISSCUSIONS

As for our output request we got results for FEM model of fuselage cabin. It include stress contour, Displacement contour.

The results of fuselage cabin just give the bench mark to the analysis of splice joint panel (flat panel). The output results are obtained and tabulated above for different pressure cycles. The stress contour and displacement contour as shown in below figures

Output Results of Fuselage Cabin

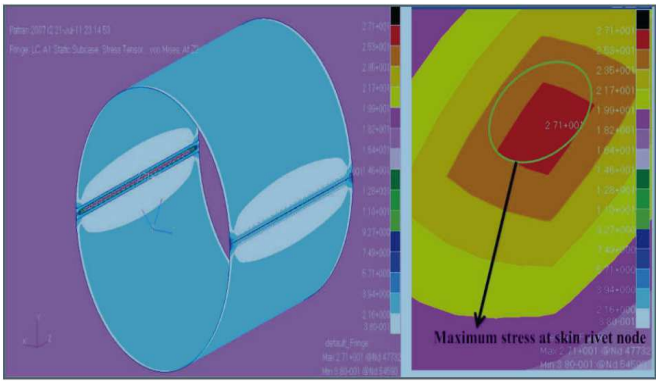

Figure 3.1: Shows at Thickness Z2 the Static Stress of Von Mises Stress Tensor Contour and Maximum Stress Location Contour

The maximum von mises stress obtained for the higher load case of 9PSI is 27.1 kg/mm2 (Node ID:47732) which is less than the ultimate stress of 40kg/mm2 and is acting on skin part of the fuselage cabin.

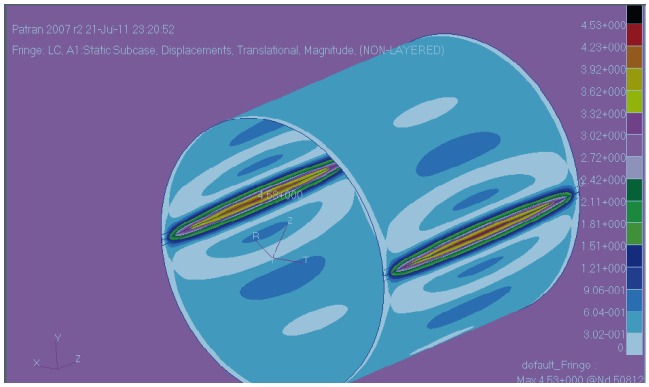

Figure 3.2: Shows the Static Displacement Contour

The maximum displacement for the load case 9PSI is 4.53mm which is at tip of the skin (node ID:50812).

Table 7: Shows the Output Results of Fuselage Cabin for Different Pressure Loads

Pressure in PSI	Pressure 'kg/mm^2'	Von mises stresses at thickness ' kg/mm^2'		Displacement 'mm'	Node ID	Beam (rivet) stresses maximum combined 'kg/mm^2'
		Z1	Z2			
6	0.00422	10.8	18.1	3.02	47731	22.9
6.5	0.00457	11.7	19.5	3.27	47731	24.8
7	0.00493	12.7	21.1	3.53	47731	26.8
7.5	0.00528	13.6	22.6	3.78	47731	28.7
8	0.00563	14.5	24.1	4.03	47731	30.6
8.5	0.00598	15.4	25.6	4.28	47731	32.5
9	0.00633	16.3	27.1	4.53	47731	34.4

Output Results of Splice Joint Panel (Butt Joint Flat Panel)

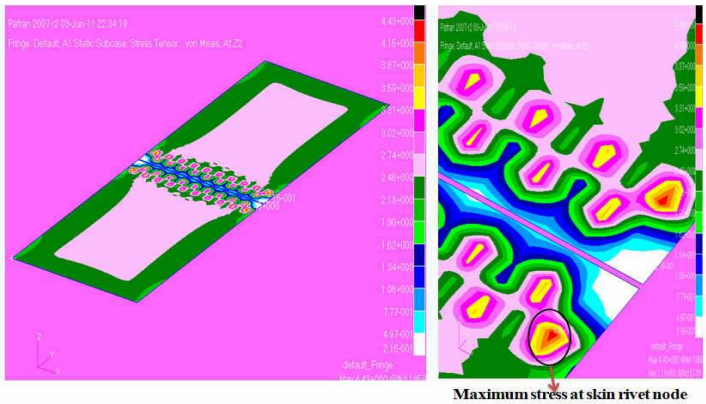

Figure 3.3: Shows at Thickness Z2 the Static Stress for Von Mises Stress Tensor and Maximum Stress Location

The maximum von mises stress obtained for the higher load case of 9PSI is 5.69kg/mm2(Node ID:1858) which is less than the ultimate stress of 40kg/mm2 and is acting on skin plate of the splice joint panel.

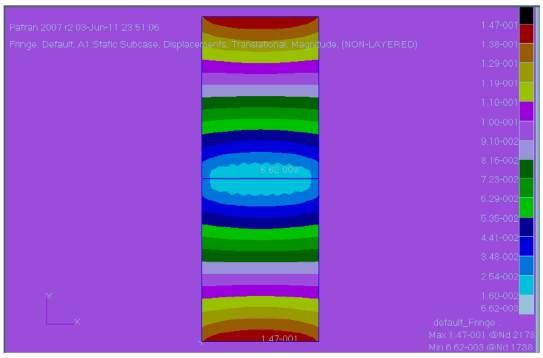

Figure 3.4: Shows the Static Displacement Contour

The maximum displacement for the load case 9PSI is 0.189mm which is at tip of the skin (node ID:2178).

Table 8: Shows the Output Results of Splice Joint Panel for Different Pressure Loads

Pressure 'PSI'	Circumferentia l stress 'σ_c'	Load 'kg'	Distribute d load 'kg/mm	Von mises stresses at thickness 'kg/mm^2		Displacemen t 'mm'
				Z1	Z2	
6	2.11	949.5	3.798	3.55	3.79	0.126
6.5	2.285	1028.25	4.113	3.85	4.11	0.137
7	2.465	1109.25	4.437	4.15	4.43	0.147
7.5	2.64	1188	4.752	4.44	4.74	0.158
8	2.815	1266.75	5.067	4.74	5.06	0.168
8.5	2.99	1345.5	5.382	5.03	5.37	0.179
9	3.165	1424.25	5.697	5.33	5.69	0.189

Output Results of Plate with Hole Analysis

The maximum von mises stress obtained for the higher load case of 9PSI 28.5kg/mm2 (Node ID:35) which is less than the ultimate stress of 40kg/mm2 and is acting on skin plate of the splice joint panel.

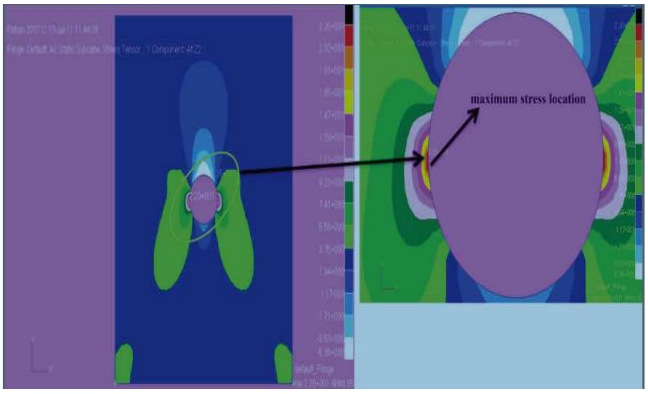

Figure 3.5: Shows at Thickness Z1 the Static Stress for Von Mises Stress Tensor and Maximum Stress Location

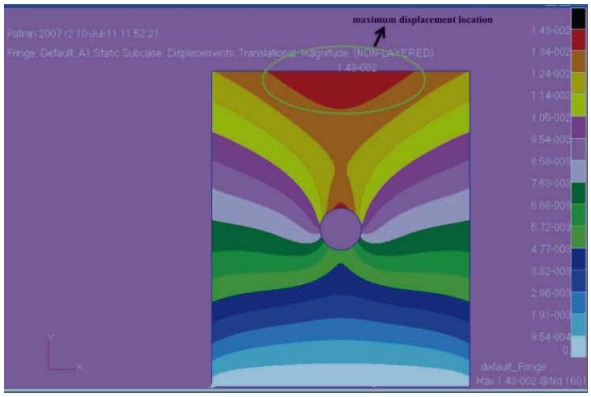

Figure 3.6: Shows the Static Displacement Contour Near the Hole and Plate End

The maximum displacement for the load case 9PSI is 0.0185mm which is at tip of the skin (node ID:1601).

Table 9: Shows the Output Results of Plate with hole for Different Pressure Loads

Pressure in PSI	Distributed load at end of the plate in kg/mm	Point load at hole= F/No of nodes in kg	maximum Stress kg/mm^2	Stress in 'Y' component	Displacement 'mm'
6	3.44	1.379	18.9	18.8	0.0122
6.5	3.735	1.492	20.5	20.4	0.0133
7	4.032	1.610	22.1	22.0	0.0143
7.5	4.32	1.724	23.7	23.5	0.0153
8	4.608	1.838	25.3	25.1	0.0163
8.5	4.896	1.953	26.8	26.7	0.0174
9	5.229	2.067	28.5	28.3	0.0185

Table 10: Shows the Maximum Local Stress Comparison by Theoretical Results with FEM Results in Plate with Hole

Sl no.	Applied pressure loads 'PSI'	σ_{max} by theoretical in 'kg/mm^2'	σ_{max} by FEM in 'kg/mm2'	% of error
1	6	16.981	18.9	11.3
2	6.5	18.385	20.5	11.5
3	7	19.837	22.1	11.4
4	7.5	21.249	23.7	11.5
5	8	22.66	25.3	11.6
6	8.5	24.07	26.8	11.3
7	9	25.559	28.5	11.5

The maximum stress is calculated from theoretical approach for different pressure cycles are tabulated above. Here we got from FEM results are higher magnitude compared to theoretical values due error in taking values in graph curves for material and theoretical assumptions, the obtained theoretical maximum stress is matched with FEM results; it showed small difference with both and error got less than 12%. hence FEM results give approximate values. The trends of both theoretical maximum stress and FEM values vary linearly with different pressure cycles as shown in above figure. Hence our

FEM results of maximum stress at rivet location are approximated values, and these values are taken for fatigue analysis at highly stressed rivet.

Maximum Stress in the Tongue

The stress distribution without considering the fork is shown in Figure. This Figure shows that the maximum stress induced in the lug joint was 45.6kg/mm^2 for Al 7075 T6 Maximum stress obtained was much below the yield stress of the material used for lug joint.

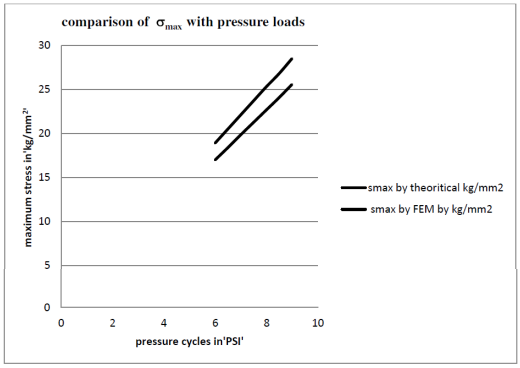

Figure 3.7: Shows for Theoretical Values and FEM Values of Maximum Stress in Element

Fatigue Life Calculation Results

Table 11: Shows the Number of Cycles to Failure from the Graph and Damage Accumulated from Miner's Formula

Pressure in psi	Applied no of cycles 'n_i'	No of cycles to failure from the graph 'N_i'	Damage accumulated from miner's formula 'd'
6	14000	9.25E+5	0.0151
6.5	7500	7.75E+5	0.00967
7	4500	3.25E+5	0.0138
7.5	1800	1.75E+5	0.0102
8	1200	8.5E+4	0.0141
8.5	500	7.75E+4	0.00645
9	500	4.75E+4	0.0105

From results of fatigue analysis for different pressure cycles got the damage fraction is less than unity. According to Palmgren-Miner linear damage rule when the damage fraction is less than unity the material is safe, often satisfactorily for failure is predicted. For different amplitude stress we got damage fraction less than unity so the material is safe. Hence satisfactorily for failure is predicted. The damage at which failure is expected to occurs when the damage fraction is equal to 1.

A typical S-N curve is plotted based on the numerical results of material 2024 T351 aluminium alloy as shown in below figure.

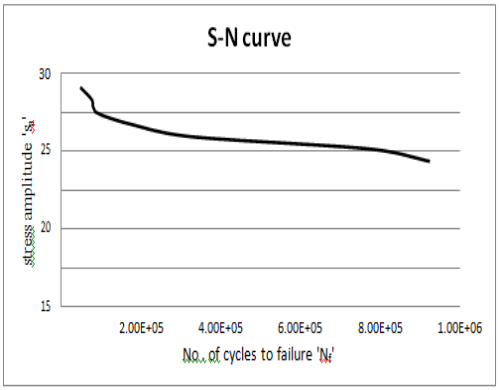

Figure 3.8: Shows the Plot of S-N Curve for Different Pressure Loads

The S-N curve for aluminum alloy 2024-T351 material for different pressure cycles sketched in figure. It shows the material response to cyclic loading commonly observed. The nonferrous alloys do not exhibit an asymptote, and the curve of stress versus life continues to drop off indefinitely. For such alloys there is no fatigue limit, and failure as a result of cyclic load is only a matter of applying enough cycles, all materials however, exhibit a relatively flat curve in the long life range. To characterize the failure response of aluminum alloy 2024-T351 for in our design loads in the finite life range, the term fatigue strength at a specified life. Above plotted S-N curve shows the fatigue damage at a given design life. Fatigue damage is defined as the design life divided by the available life.

From above S-N curve stress amplitude of 18.733 and the number of cycles at failure 'Nf'is 4.75E+4 below which the material as longer live i. e. infinite life. The fatigue life Nf for our designed loads is the number of cycles of stress of a specified character that a given specimen sustains before failure of a specified nature occurs

CONCLUSIONS

- The maximum von mises stress obtained for the higher load case of 9PSI is 27.1kg/mm2) which is less than the ultimate stress of 40kg/mm2 and is acting on skin part of the fuselage cabin.
- The maximum von mises stress obtained for the higher load case of 9PSI is 5.69 kg/mm2which is less than the ultimate stress of 40kg/mm2 and is acting on skin plate of the splice joint panel.
- The maximum von mises stress obtained for the higher load case of 9PSI is 28.5kg/mm2which is less than the ultimate stress of 40kg/mm2 and is acting on skin plate of the splice joint panel

REFERENCES

1. *G. S. Campbell and R. Lahey "A survey of serious aircraft accidents involving fatigue fracture" National Research Council of Canada, Int J Fatigue Vol 6 No 1 January 1984, ISBN 0142-1123/84/010025-06 © 1984 Butterworth & Co Ltd.*
2. *J. Schijve "Fatigue of aircraft materials and structures" Faculty of Aerospace Engineering, Delft University of Technology, the Netherlands, Fatigue1994 volume 16 number1, ISBN 0142-1123/94/01/0021-12 © 1994 Butterworth-Heinemann Ltd.*
3. *R. J. H. Wanhill, M. F. J. Koolloos "Fatigue and corrosion in aircraft pressure cabin lap splices" National Aerospace Laboratory NL-1009 BM Amsterdam, the Netherlands, International Journal of Fatigue 23 (2001) S337–S347, © 2001 Elsevier Science Ltd.*
4. *M. R. Urban "Analysis of the fatigue life of riveted sheet metal helicopter airframe joints" Structures Research Department, Sikorsky Aircraft Corporation, USA, International Journal of Fatigue 25 (2003) 1013–1026, © 2003 Elsevier Ltd.*

5. *Rajaraman, R., Hariharan, G., & Sripathy, B. An Efficient Hybrid Analytical Approach, To Film Pore Diffusion Model Using Wavelets.*
6. *A. M. Brown, P. V. Straznicky "Simulating fretting contact in single lap splices" Department of Mechanical and Aerospace Engineering, Carleton University, Canada, International Journal of Fatigue 31 (2009) 375–384, 2008, © Elsevier Ltd.*
7. *Lucas F. M. Silva, J. P. M. Gonc¸alves, F. M. F. Oliveira, P. M. S. T. de Castro "Multiple-site damage in riveted lap-joints: Experimental simulation and finite element prediction" Department of Mechanical Engineering and Industrial Management, University of Porto, Portugal, International Journal of Fatigue 22 (2000) 319–338, © 2000 Elsevier Science Ltd.*
8. *Agboola, R. Analytical Interpretation Of Geomagnetic Fieldanomaly Along The Dip Equator.*
9. *Elzbieta Szymczyk, Jerzy Jachimowicz, Grzegorz Slawinski, Agnieszka Derewonko*
10. *"Influence of technological imperfections on residual stress fields in riveted joints" Military University of Technology, Poland, Procedia Engineering 1 (2009) 59–62, © 2000 Elsevier Science Ltd.*
11. *Roberto Galatolo, Karl-Fredrik Nilsson "An experimental and numerical analysis of residual strength of butt-joints panels with multiple site damage" Department of Aerospace Engineering, University of Pisa, Italy. European Commission. Joint Research Centre, Institute for Advanced Materials, the Netherlands, Engineering Fracture Mechanics 68 (2001) 1437-1461, © 2001 Elsevier Science Ltd.*
12. *R. L. Veldman, J. Ari-Gur, C. Clum, A. DeYoung and J. Folkert "Effects of prepressurization on blast response of clamped aluminum plates" Department of Physics and Engineering, Hope College, USA, Department of Mechanical and Aeronautical Engineering, Western Michigan University, USA, International Journal of Impact Engineering 32 (2006) 1678–1695, © 2005 Elsevier Ltd.*
13. *Horsfall, O., Uko, E., & Davies, D. Statistical Analysis On Corrected Well-Log Derived Temperatures In South-Eastern Niger Delta.*
14. *Min Liao, G. Shi, Y. Xiong "Analytical methodology for predicting fatigue life distribution of fuselage splices" Structures, Materials and Propulsion Laboratory, Institute for Aerospace Research, National Research Council Canada. International Journal of Fatigue 23 (2001) S177–S185.*
15. *Sergey Shkarayev, Roman Krashanitsa "Probabilistic method for the analysis of widespread fatigue damage in structures" Department of Aerospace and Mechanical Engineering, The University of Arizona, Tucson, AZ 85721-0119, USA, International Journal of Fatigue 27 (2005) 223–234, © 2004 Elsevier Ltd.*
16. *Jaap Schijve "fatigue damage in aircraft structures, not wanted, but tolerated"? Delft University of Technology, Faculty of Aerospace Engineering Kluyverweg 1, 2629 HS, the Netherlands.*